Experimental and numerical investigation of the speed-no-load instability of a low specific speed pump-turbine with focus on the influence of turbulence models

IOP Conf. Series: Earth and Environmental Science **240** (2019) 082005 doi:10.1088/1755-1315/240/8/082005

Experimental and numerical investigation of the speed-no-load instability of a low specific speed pump-turbine with focus on the influence of turbulence models

Sabri Deniz, Armando Del Rio and Ernesto Casartelli

Lucerne University of Applied Sciences & Arts, Institute of Mechanical Engineering and Energy Technology, Technikumstrasse 21, CH-6048 Horw, SWITZERLAND

E-mail: sabri.deniz@hslu.ch

Abstract A reduced scale model of a low specific speed pump-turbine with 7 runner blades and 20 guide vanes is experimentally and numerically investigated. Main goal is to identify the onset, origin, and development of flow instabilities. The four-quadrant characteristic of the pump-turbine is experimentally determined. The focus of this paper is on the turbine mode operation at off-design conditions involving runaway and the "S-shape" turbine characteristic. 3D, unsteady numerical simulations are performed using the CFD codes ANSYS-CFX and an in-house code. The computational domain includes the entire flow passage from the spiral casing inlet to the draft tube exit. For turbulence modeling the SST k-ω, standard k-ε, and BSL EARSM models are applied. The numerical results at two guide vane openings (20° and 6°) and different operating points at each guide vane opening are compared to the experimental results. The comparisons between the CFD predictions and experimental data shows that the CFD predictions of all turbulence models are in good agreement with the experimental data for 20° guide vane opening whereas for the 6° guide vane opening, which is critical for the synchronization, only the k-ε and BSL EARSM turbulence models are showing a reasonable agreement with the experimental data. Based on the detailed analysis of the experimental data and CFD results focusing especially on the flow features in the vaneless space and at the runner inlet, the onset and development of the flow instabilities are explored.

1. Introduction

Reversible pump-turbines add versatility to the electricity market because they can be switched between pump and turbine operations within a short time. In turbine mode, they are used to cover the peak energy demand and in pump mode they store the excess energy. Accordingly, reversible pump-turbines allow more flexibility and stabilization of the power grid. Due to the increased production of renewable energy such as wind and solar energy, balancing the energy supply and demand becomes more difficult. Thus, pump-turbines are gaining additional importance for energy storage, grid regulation, and peak energy production. In order to balance the changes in electricity production and consumption, pump-turbines need to switch quickly between pump and turbine modes with extended operation under off-design conditions.

The emphasis on the design of the more sensitive pump flow however often leads by pump-turbines to stability problems in speed-no-load or turbine brake operations. This results from unstable pump-

turbine characteristics that are responsible for oscillation in hydraulic systems. For reversible pump-turbines, the characteristic curves exhibit an S-shape in the turbine, turbine brake and reverse pump regions. Pump-turbines are synchronized with the electrical grid at speed no load, a procedure which will be delayed in case of system oscillations excited by the unstable behavior of the pump-turbine at runaway. The consequences are high mechanical stresses and longer switching times or even a complete inability to synchronize the pump-turbine with the power grid. Another critical operation is the load rejection where within short time, the operating point of the turbine moves from full load to no load and may overshoot to turbine brake in the case that the guide vanes and inlet valves do not close rapidly. If the pump-turbine characteristic is unstable in this range, low frequency system oscillations may arise, which might damage the hydraulic system elements. The requirements of a stable and reliable pump-turbine operation under continuously expanding operating ranges challenges the hydraulic design and requires new developments. The reason for the instability is related to complex flow patterns in the pump-turbine, but the details of the stability onset and development are not yet fully understood. Previous research at the Lucerne University of Applied Sciences (HSLU) analyzed the instabilities of a medium specific speed pump turbine and the unstable characteristics were correlated with vortices forming in the runner channel close to the leading edge [1].

The focus of this research is in the prediction of the pump-turbine characteristics and the explanation of the physical phenomena that are intrinsic to pump-turbine instability (prediction and detection of the onset of instabilities, determination of their origin, and understanding their development) by applying CFD simulations. The goal is not only enhancing the operating range of pump-turbines beyond the current stability limits, but also allowing establishment of design guidelines for stable pump-turbine designs based on the newly obtained knowledge of the cause of pump-turbine instabilities. Achieving these goals require a CFD methodology, which can adequately predict the characteristics and flow features of pump-turbines especially at off-design conditions.

An accurate numerical prediction of pump-turbine instabilities becomes crucial and numerical accuracy plays a major role in modern pump turbine design in order to analyze and understand the mechanisms leading to the flow instabilities. It is advantageous to determine onset and intensity of the instabilities in the S-region properly before proceeding with the model tests. This study aims at predicting the S-shaped characteristics of a pump-turbine by using different numerical approaches, especially applying different turbulence modes. CFD (Computational Fluid Dynamics) simulations of a low specific speed reversible pump-turbine operating at design and off-design conditions are performed using an in-house CFD tool (a modified version of OpenFOAM) and the commercial code ANSYS CFX. The results of CFD simulations are compared with the experimental data obtained from the measurements at the same institution.

2. Speed no load instability: The S-shaped characteristics in the turbine mode

The operating point (OP) of a pump-turbine in turbine mode switches back and forth between turbine (brake) and reverse pump modes, if the characteristics in this speed no load region has an S-shape. Such an S-shaped characteristic is depicted in Figure 1. For the occurrence of instabilities is the slope of the characteristics crucial. A positive slope of $dKcm_1/dKu_1 > 0$ and $dKm_1/dKu_1 > 0$ indicates an unstable branch in characteristics.

The definitions of the dimensionless Ku_1, Kcm_1 and Km_1 coefficients are:

$$Ku_1 = \frac{\pi n D_1}{60\sqrt{2gH}} \; ; \; Kcm_1 = \frac{4Q}{\pi {D_1}^2 \sqrt{2gH}} \; ; \; Km_1 = \frac{8M}{\pi \rho g H {D_1}^3}$$

- n = rotational speed of the pump-turbine [rpm]
- D_1 = runner diameter [m]
- g = 9.81 [m/s^2] (gravity acceleration)
- Q = flow rate [m^3/s]
- H = pump-turbine head [m]
- M = torque on the runner [Nm]

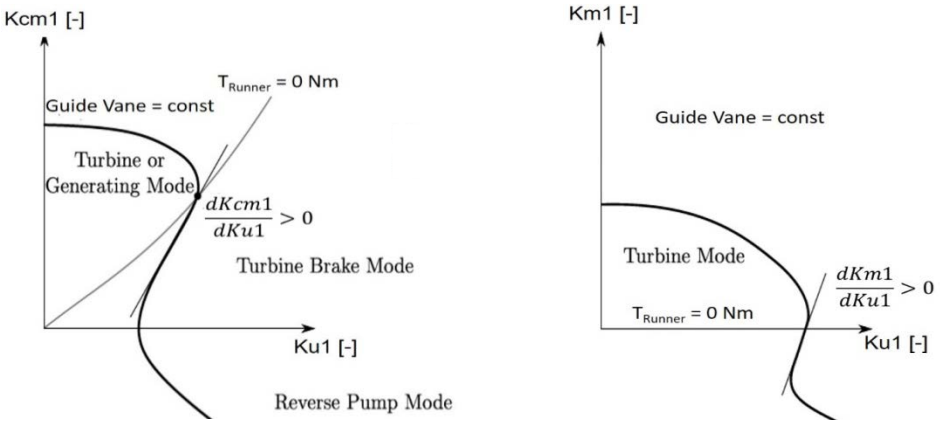

Figure 1. S-shaped characteristic ((a): discharge, (b): torque) of a pump-turbine at a constant guide vane opening.

The slope of the characteristic gives a necessary but not sufficient condition for the instability of the hydraulic system. Further criteria lie in the elasticity, inertia and the amount of energy dissipated in the system. Once the energy transferred is larger than the dissipated one, the system becomes self-excited.

3. Pump-turbine model

The specifications of the model pump-turbine investigated are listed in Table 1, where D_1 is the runner diameter at the pressure side (i.e. inlet at the turbine mode operation). The flow in the model pump-turbine was simulated at 6°and 20° Guide Vane Opening (GVO)'s.

Table 1. Pump-turbine model characteristics.

Parameter	Value
Number of runner blades	7
Runner diameter D_1 [mm]	422
Rotational speed n [rpm]	1500
Number of guide vanes	20
Specific Speed $n_q = nQ^{(1/2)} H^{-(3/4)}$	26
6° GVO: synchronization speed	
20° GVO: best efficiency point (BEP)	

4. Numerical analysis

Numerical Setup, Grid, Boundary Conditions & Turbulence Models

The computational domain represents the entire pump-turbine and consists of a spiral case, stay vanes, guide vanes, runner and draft tube (Figure 2 (a)). The draft-tube outlet is extended to a certain length (except for load rejection simulation) for smoothing the swirling flow and achieving easier convergence. Grids for different domains were generated by software ANSYS ICEM (original model) and by Pointwise (grid sensitivity study). The grid specifications for the original model can be found in Table 2. Special refinements were applied in the runner and guide-vanes domains. 3D, steady and unsteady numerical simulations are performed using the CFD codes ANSYS-CFX and an in-house code, which is a modified OpenFOAM version. More information about the in house code can be found in [2].

The boundary conditions were defined as follows: at the spiral case inlet the mass flow rate, turbulence intensity of $I_T = 0.05$ and a viscosity ratio (ν_t/ν) of 10 are specified. An area-averaged static pressure of $p = 0$ is prescribed at the draft tube outlet. Exit opening condition allows re-entering of flow at the outlet and thus reduces numerical oscillations. The walls are defined as no-slip walls. Considering the rotating runner domain, a constant rotational speed n is predefined for all computations. The individual hydraulic components are numerically coupled by General Grid Interfaces (GGIs) in ANSYS-CFX and by Arbitrary Mesh Interfaces (AMIs) in the in-house code. These algorithms also allow transient rotor-stator interactions which are needed to connect the rotating runner with its surrounding stationary domains. Maximum simulation duration corresponds to ca. 20 runner revolutions. All evaluated quantities are averaged over a period of ca. 10 runner rotations. The time resolution during the transient simulations was 1/20 of a runner-channel rotation, which corresponds to ca 2.6° per time step. During the numerical simulations, the results of steady RANS simulations were used as the initial flow field for the transient simulations. The time-step was set to 0.29 ms, and the maximum number of iterations per time-step was set to 10 with the convergence criteria of residual at each time-step was in the order of 10^{-5}.

Based on a comprehensive analysis of the literature about pump-turbine CFD simulations (see section 6), the SST k-ω, standard k-ε, and BSL EARSM turbulence models are applied.

Table 2. Grid specifications (ICEM) for the original model.

	Total	Spiral-Case	Guide Vanes	Runner	Draft-Tube
Mesh size (Hexahedron)	5.8 Mio.	1.5 Mio.	1.5 Mio.	2.3 Mio.	0.5 Mio.
Min. Angle [°]	13.1	13.1	39.7	24.1	42
Max. Aspect Ratio	777	777	139	403	139
Max. Volume Change	79.5	69.1	2.4	79.5	2.6
Min. Determinant	0.17	0.17	0.45	0.52	0.63

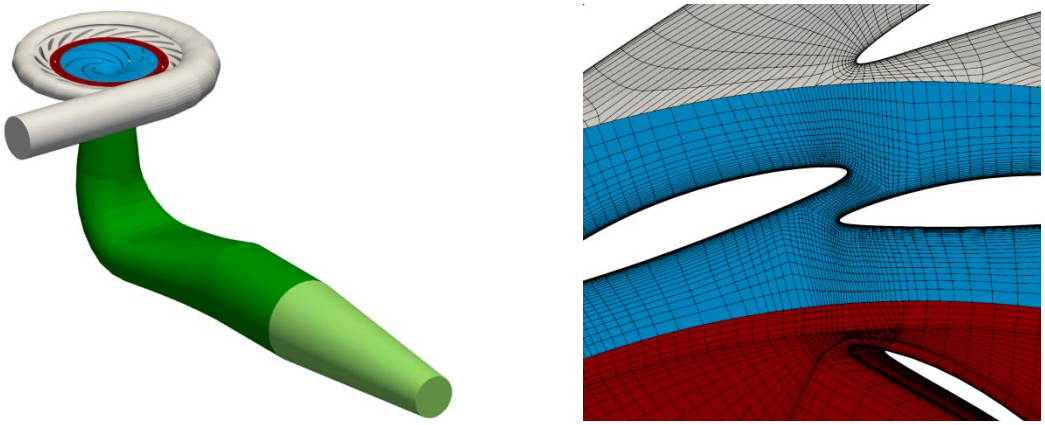

(a) (b)

Figure 2. Computational grid used for the CFD simulations with spiral case, guide-vane, runner and draft tube zones highlighted (a) and zoom in the guide-vane/runner interface zone (b).

5. Results

5.1. Transient simulations at fixed operating points

5.1.1. Performance of different turbulence models: Mean values. Only the results of the transient CFD simulations are presented. Figure 3 is a comparison of the pump-turbine Kcm_1-Ku_1 (discharge) and Km_1-Ku_1 (torque) turbine mode characteristics between measurements and in-house code CFD predictions for two guide vane openings GVO 6° & 20°. Shown in all Kcm_1-Ku_1 figures is also the runaway line,

i.e. the curve where the runner-torque is equal to zero. The turbine discharge characteristic at a constant GVO starts from part load operation, moves through BEP and then through runaway along the S-shaped curve down to turbine brake and reverse pump modes. Important point with regard to the pump-turbine numerical simulations is the ability of the CFD simulations in capturing the curvature (S-shape) of the curve with the change of the slope as depicted in Figure 1. The comparisons in Figure 3 show good agreement between the experimental data and k-ε CFD predictions for both GVO's. The SST k-ω CFD simulation is also capable to predict GVO 20° test data, but fails for the GVO 6° as can be better seen in Figure 4.

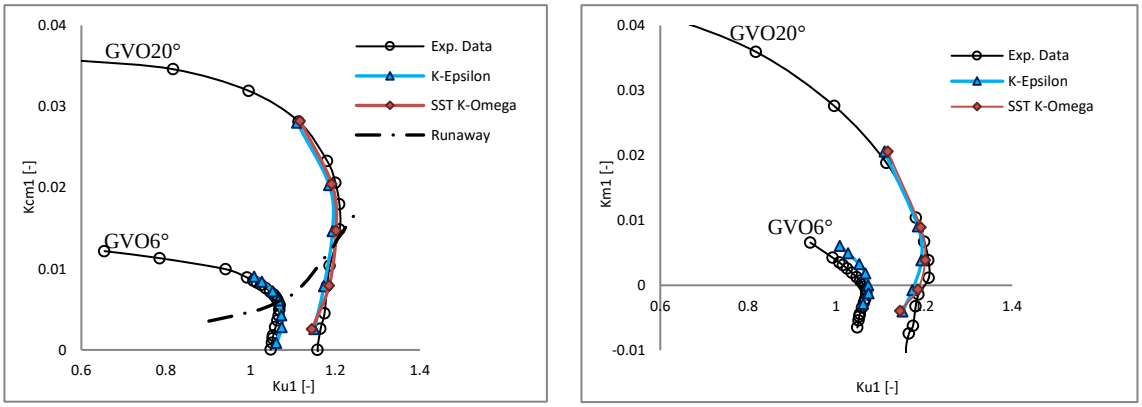

(a) (b)

Figure 3. Comparison of the pump-turbine characteristics ((a): discharge, (b): torque) between measurement and CFD (in-house code, k-ε & SST k-ω) for GVO 6° & 20°.

With regard to the speed no load instability and synchronization of the pump–turbine GVO 6° is important. Figure 4 depicts the CFD prediction of the Kcm_1-Ku_1 characteristic for GVO 6° in the S-region and comparison with the experimental data. The CFD calculations are carried out with the application of the following turbulence models: k-ε, SST k-ω, SST k-ω with curvature correction, and BSL EARSM. CFD data for both solvers i.e. CFX and in-house code are presented in Figure 4 and comparisons of the simulations between the in-house code and ANSYS CFX indicate no detectible difference in results for the same operation point. Real effect on the CFD predictions has the turbulence model.

As can be seen in the Figure 4, the SST k-ω turbulence model cannot calculate the S-shaped characteristic for GVO 6°. Important point is not only the difference between the predicted and measured values, but also the incapability of the SST k-ω model of predicting the instability (i.e. positive slope of the Kcm_1-Ku_1 curve in S-region) at speed no load conditions. The curvature correction did not bring any improvement in the prediction of the SST k-ω model. Although the accuracy in turbine brake mode is not very good the k-ε turbulence model produces acceptable results and the best result is achieved with the BSL EARSM turbulence model concerning the accuracy as well as reflecting the S-shape (including the slop change) of the S-curve. BSL EARSM seems to be a suitable choice to reproduce the characteristic and flow features in the pump-turbine investigated at low GVO's.

5.1.2. Performance of different turbulence models: Fluctuating behavior. According to the Figure 4, the SST k-ω turbulence model cannot predict the instability behavior of the pump-turbine at GVO 6°. In Figure 5, the in-house code CFD predictions with the SST k-ω and k-ε models are compared with respect to the oscillations of the solutions for three different operating points. During the transient CFD calculations in the S-region, the Ku_1 values oscillates around its mean value and the magnitude of these oscillations for the SST k-ω model predictions are significantly smaller in comparison to both the k-ε and the EARSM models. The variable δKu_1 in Figure 5 (a) is defined as $Ku_{1,max} - Ku_{1,min}$. Figure 5 (b) shows the magnitude of the oscillations for the discharge characteristic. The flow field calculated by the

SST k-ω model in the S-region of instability oscillates considerable less than the calculation with the k-ε model. Similar difference between SST k-ω model and k-ε model simulations is also observed during the load rejection simulation of the same pump-turbine model (see section 5.2).

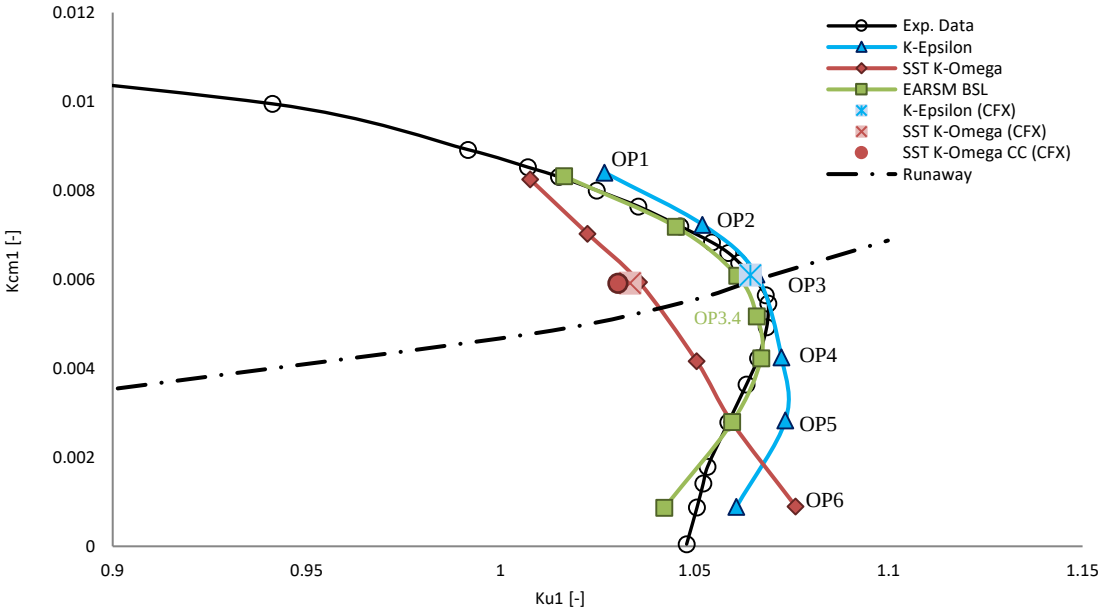

Figure 4. Influence of the turbulence model on the predictions of the discharge characteristic in S-region for GVO 6° (Data are in house code simulations unless specified otherwise in parenthesis).

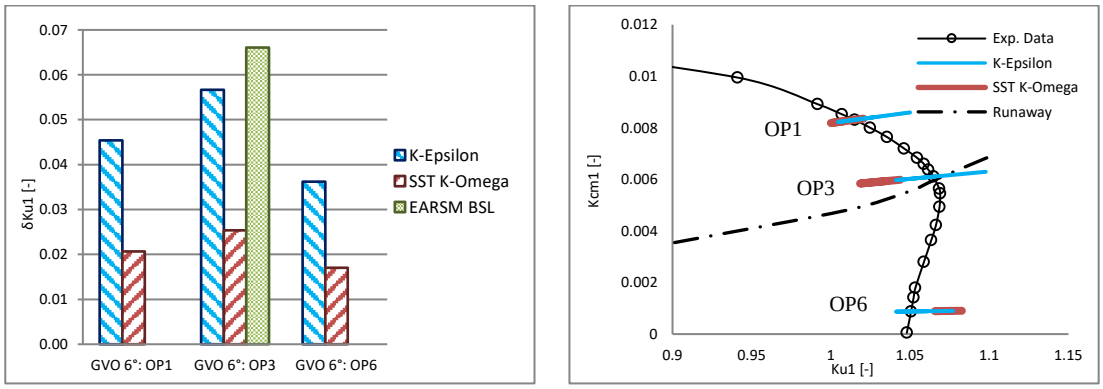

(a) (b)

Figure 5. Oscillatory behavior of different simulation models for GVO 6°.

5.1.3. Grid independence study. Grid independence studies were conducted with several different mesh refinement levels. Two types of grid dependency investigations were carried out. A global grid study in which the boundary layer grid was not influenced and a separate grid refinement of the boundary layer. The investigated grid resolutions are summarized in Table 3.

Table 3. Grid independence study (RU: Runner, GV: Guide Vane).

	GV Mesh Size	RU Mesh Size	GV $y+_{average}$	RU $y+_{average}$
Refinement 1	4.7 Mio.	2.3 Mio	19	20
Refinement 2	2x Refinement 1	2x Refinement 1	19	20
Refinement 3	2x Refinement 2	Refinement 2	19	20
Low Reynolds Mesh	11.8 Mio.	11 Mio.	0.8	1.7

The mesh refinement study was carried out for each turbulent model separately. Different levels of grid refinements shown in Table 3 did not influence the global parameters such as the turbine head (only 0.2 % difference between fine and "coarse" grids). Figure 6 shows the results of the mesh refinement studies for the k-ε turbulence model. Overall and local grid refinements (refinement near the wall regions and refinement of the runner and guide vane grids) did also not have any noticeable impact on the calculated Kcm_1-Ku_1 values as shown in Figure 6a and Figure 6b, which is an enlarged version of the Figure 6a. Considering the numerical accuracy and computation time, for all simulations the original model, inclusive the same mesh (Table 2) was used.

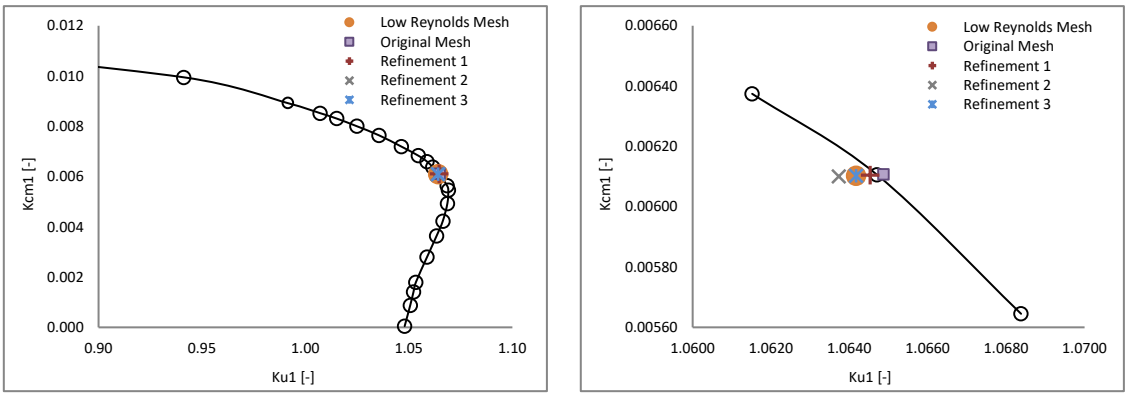

(a) (b)

Figure 6. The effects of mesh refinement for simulations with k-ε turbulence model (in house code).

5.2. Load rejection (dynamic simulations)

A 3D-CFD simulation is conducted to investigate and model the load rejection processes of the model pump-turbine starting from a stable operating condition at GVO 24° and at design speed . The load rejection simulation includes one-way FSI (Fluid Structure Interaction) for the GV motion, which setting's changes from 24 to 6 degrees. The boundary conditions were taken from the 1D transient system simulations, imposing the resulting angular velocity, GV position and mass-flow as a function of time (see references [3] and [4] for more detail). The operating conditions extend through the S-shape region of the turbine characteristic into the turbine-brake and reverse-pump domain as can be seen from the Kcm_1-Ku_1 representation in Figure 7 (a). Changes of turbine head and torque over time during the load rejection simulation are also depicted in Figures 7 (b) respective (c) for the k-ε and SST k-ω models. Both head and torque changes from the load rejection simulation follow the 1D prediction over the complete simulated time-frame, but there is a big difference in the calculated magnitude of oscillations between two turbulence models. According to the Figure 7 (a), there are large oscillations in the GVO 6° region between 15 and 25 seconds of the load rejection simulation (the turbine is oscillating along the S-shaped GVO 6° characteristic). k-ε simulation depicted in Figure 7 (b) & (c) reflects these oscillations of high magnitude in head and torques curves whereas SST k-ω model predictions are not able to reflect these oscillations between 15-25 seconds. The SST k-ω simulation produces a large dissipation in the vaneless space between GV and runner, thus damping the instabilities even in the S-

region. Large oscillations of the head or torque signals are indicators of the instabilities on the pump-turbine, which are mostly triggered by the vortex structures in the vaneless space (or runner inlet) and play an important role for unstable operating conditions.

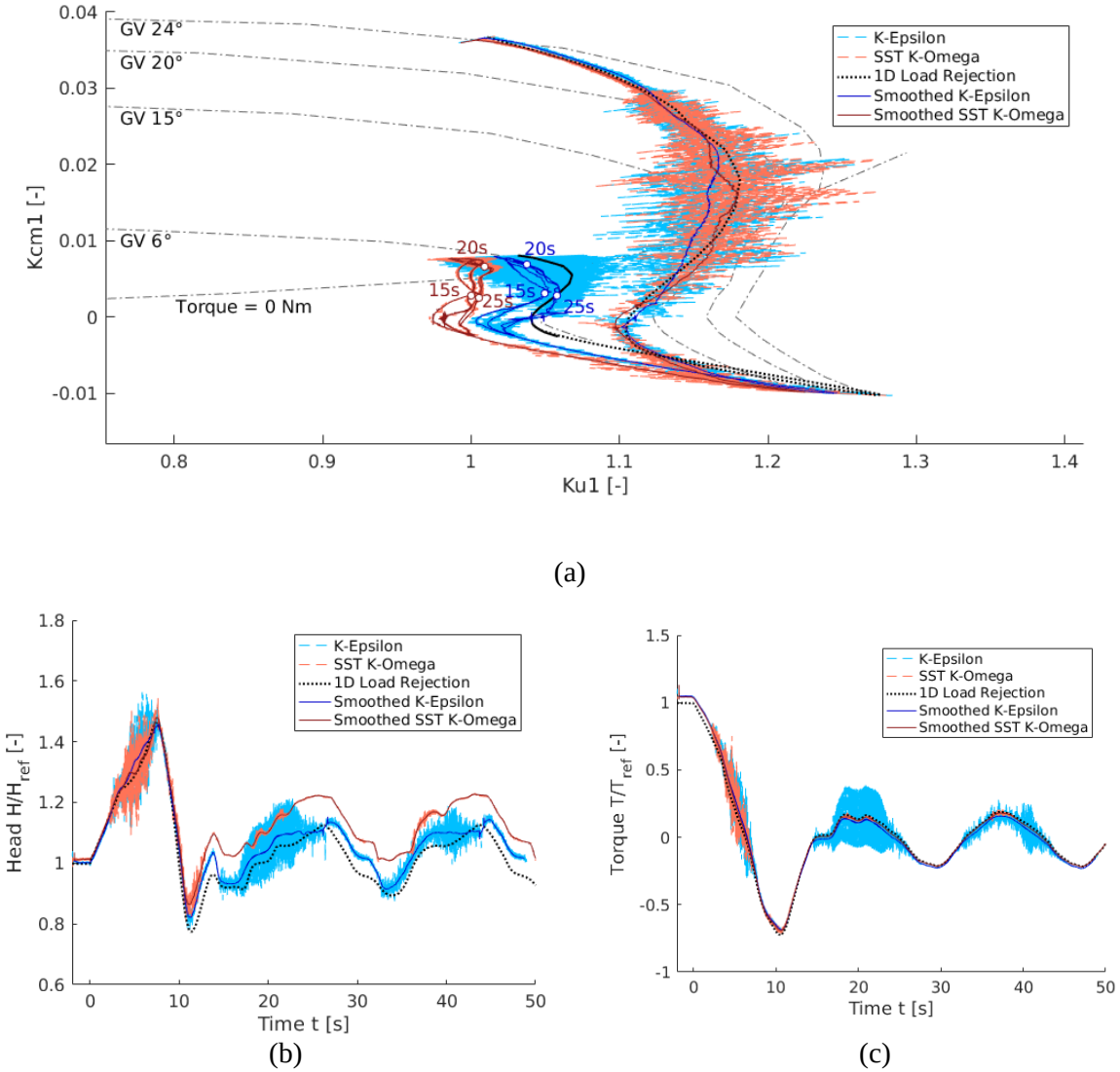

Figure 7. Load rejection CFD results (in-house solver) with the k-ε and SST k-omega models.

5.3. Analysis of the flow patterns for simulations with different turbulence models

In order to further analyze the reasons of the different predictions by the SST k-ω and k-ε models, contour plots of the radial velocity on the runner midplane (top part of the Figure 8) and on a circumferential plane between hub and shroud in the vaneless space prior to the runner inlet (bottom part of the Figure 8) are plotted. As can be seen on the contour plots (Figure 8) there is a strong vortex driven backflow (red color) at the inlet of the runner observed at all channels simultaneously in case of SST k-ω model, whereas the k-ε model shows this behavior at the runner inlet only at certain channels. The vortex structures predicted by the SST k-ω model are very "stable" and predicted by the k-ε are not only oscillating but also changing in the size. There is vortex formation and-destruction for the k-ε case

and there are positions along the runner inlet where some of the channels are free of vortices, so that the flow can enter the runner. The formation and vanishing of the vortices seems to produce the large head and torque oscillations observed in Figure 7 (b) & (c). Similarly, the radial velocity distribution in the vaneless space shows a backflow region (red color) for each runner channel, which spans almost over the complete width and exists at all runner channels for the SST k-ω model calculation. Same backflow region for the k-ε model simulation show differences in circumferential direction with respect to the individual runner channels.

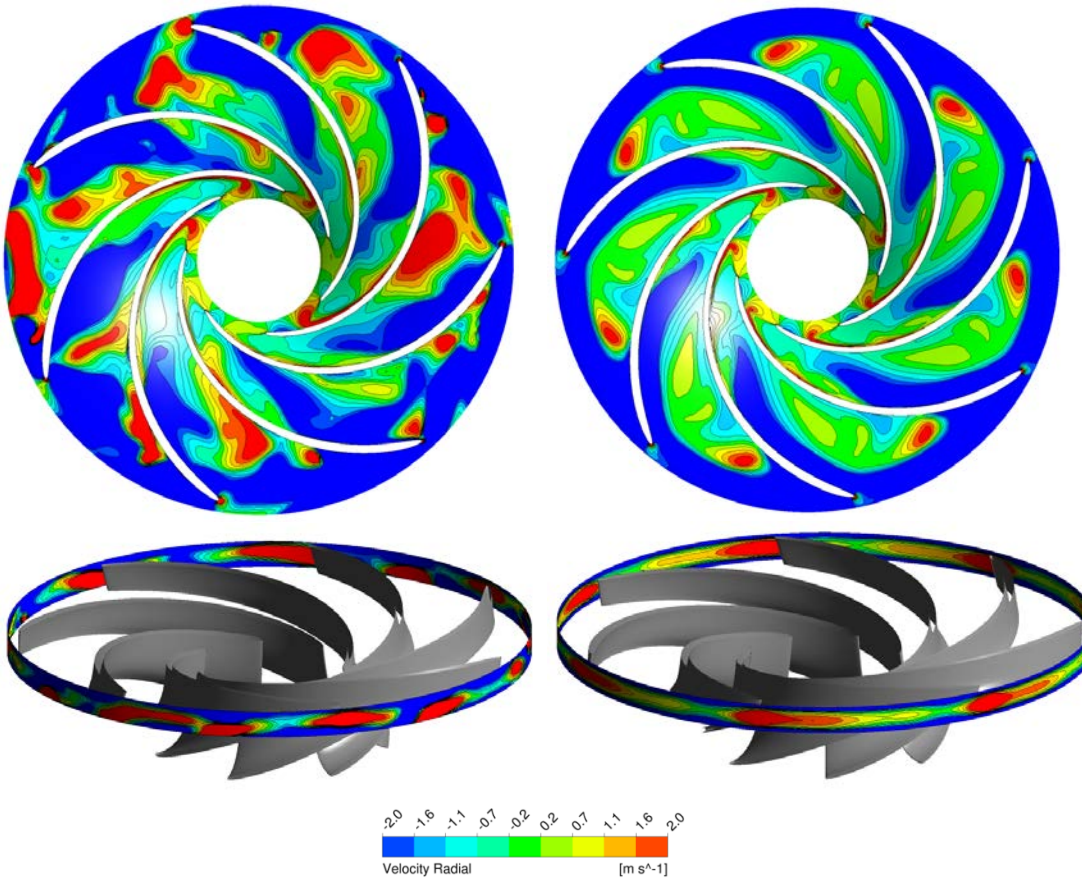

Figure 8. Contour plots of the radial velocity on the midplane (top part) and at the runner inlet (bottom part). Left figures: k-ε model, Right figures: SST k-ω model (both CFX simulations).

6. Comparisons with similar CFD simulations from the literature

Several works have been published in the literature, which aims precisely at computing the characteristics of pump-turbines in turbine mode, including the sloping gradient of the S-shape and investigating the flow phenomena at off-design conditions. In addition to the CFD solvers used (ANSYS CFX, ANSYS Fluent, and OpenFOAM) main differences in the CFD simulations are in the turbulence models: SST k-ω, SAS-SST, standard k-ε, RNG k-ε, four-equation v2-f model, and BSL EARSM turbulence models are applied.

In general the CFD results are in good agreement with the experimental data in predicting the characteristics for high guide vane angles i.e. guide vane angles at or near BEP, ([5], SST k-ω, medium n_q pump-turbine) ([6], SST k-ω, high n_q pump-turbine), ([7], SAS, medium n_q pump-turbine) ([8], RNG k-ε), ([9], SAS, low, medium, and high n_q pump-turbines) but the difficulties increase when calculating the S-shaped characteristics at low guide vane angles near synchronization, where especially the SST k-

ω model has problems in predicting the characteristics. According to [10], (medium n_q pump-turbine) v2-f model can be used to simulate characteristics of pump-turbine in the whole guide vane opening range and the SST k-ω model can only be used for large guide vane openings. A detailed CFD study ([11], with SST k-ω, standard k-ε, BSL EARSM, and v2-f models) on three different pump-turbines, also concludes the incapacity of the SST k-ω model to accurately determining S-shaped characteristics. [12] (SST k-ω low n_q pump-turbine) seems an exception, where SST k-ω model was able to predict the S-shaped characteristics at the GVO's of 6°, 21° and 24°.

Simulations with low n_q pump-turbines are in general more challenging. [13] (low n_q pump-turbine) shows good prediction of the S-characteristics with the k-ε model. [14] uses detached eddy simulation (DES) and found better agreement with the test data than using the SST k-ω model. [15] uses SAS-SST model and successfully calculated the characteristics at different GVO's. SAS-SST model introduces the von Karman length-scale into the turbulence scale equation and this information allows the SAS-SST model to dynamically adjusting to the resolved structures in the unsteady Reynolds Averaged Navier-Stokes simulation, which means a LES-like behavior in the unsteady flow regions. At the same time, the model provides standard RANS capabilities in stable flow regions.

7. Conclusions

This work aims at developing a CFD methodology to accurately predicting S-shaped characteristics of the reversible pump-turbines with an acceptable computational cost and power. The study especially reveals the influence of the turbulence model on computed results.

In general, the unsteady CFD simulations under transient operating conditions can reproduce the measured S-shaped characteristics at high guide vane angles with acceptable accuracy and supply beneficial information about the flow phenomena occurring along the S-curve.

Although the continuous development in numerical methods manifests itself in big improvements in prediction quality, CFD simulations of pump-turbines in the speed no load region with S-shaped characteristics is challenging especially at low GVOs. In this work, simulations at small guide vane angles (around 6°) with the k-ε turbulence model showed good agreement with the test data, while for the simulations with the SST k-ω model the behavior around the S-shape (and thus the instability) could not be captured. The highest accuracy is yielded for both CFD tools used Ansys CFX and in-house code with the BSL EARSM turbulence model. These results are in agreement with the published literature in this area, where BSL EARSM seems to be most suitable model to reproduce flow conditions in the pump-turbine at speed no load conditions at a reasonable computational cost and time. SAS-SST and v2-f turbulence models are not used in this work, but according to the literature survey, both models are working well at speed no load conditions, but with a significant increase in grid size and computation time.

The analysis of the flow structures at the runner inlet and in the vaneless space as well as the results of the load rejection CFD simulations show that the flow field, including the vortex structures predicted by the SST k-ω model predictions are much more "stable", than those of the predictions of the k-ε and EARSM simulations. More detailed fluid dynamic analysis of the flow field and further explanation of the speed no load instability using the CFD and test data of this low n_q pump-turbine model will be provided in a following paper.

A validated CFD methodology, which is capable of predicting the characteristics of the pump-turbines in S-region (speed no load conditions) with a reasonable computational cost and time is crucial in order to carry out design improvements by influencing the S-shape of the characteristics and thus improving the stability.

Acknowledgments
Major funding for this project was provided by the Swiss Commission for Technology and Innovation (CTI) under Grant: 17360.1 PFEN-IW and SCCER –FURIES. Additional funding and support to the project by Andritz Hydro is greatly appreciated.

References
[1] Widmer C, Staubli, T and Ledergerber N 2011 Unstable characteristics and rotating stall in turbine brake operation of pump-turbines *Journal of Fluids Engineering* **133**(4) 041101
[2] Mangani L, Buchmayr M and Darwish M 2014 Development of a novel fully coupled solver in openfoam: Steady-state incompressible turbulent flows. *Numer. Heat Transfer* B **66**(1) 1-20
[3] Casartelli E, Mangani L, Ryan O and Schmid A 2016 Application of transient CFD-procedures for S-shape computation in pump-turbines with and without FSI *IOP Conference Series: Earth and Environmental Science* **49**(4) 042008 IOP Publishing
[4] Casartelli E, Del Rio A, Schmid A and Mangani L 2017 CFD computation of transients in Pump-turbines. HYDRO 2017, Sevilla
[5] Xiao Y, Zhu W, Wang Z, Zhang J, Zeng C and Yao Y 2016 Analysis of the internal flow behavior on S-shaped region of a Francis pump turbine on turbine mode *Engineering Computations* **33**(2) 543-61
[6] Wang L, Yin J, Jiao L, Wu D and Qin D 2011 Numerical investigation on the "S" characteristics of a reduced pump turbine model *Science China Technological Sciences* **54**(5) 1259-66
[7] Jacquet C, Fortes-Patella R, Balarac L and Houdeline J B 2016 CFD investigation of complex phenomena in S-shape region of reversible pump-turbine *IOP Conference Series: Earth and Environmental Science* **49**(4) 042010 IOP Publishing
[8] Guo L, Liu J T, Wang L Q, Jiao L and Li Z F 2012 Numerical analysis on pump turbine runaway points *IOP Conference Series: Earth and Environmental Science* **15**(4) 042017 IOP Publishing
[9] Xia L, Cheng Y, You J, Zhang X, Yang J and Qian Z 2017 Mechanism of the S-Shaped Characteristics and the Runaway Instability of Pump-Turbines *Journal of Fluids Engineering* **139**(3) 031101
[10] Liu J, Liu S, Wu Y, Sun Y and Zuo Z 2012 Prediction of "s" Characteristics of a Pump-Turbine with Small Opening Based on V2F Model *International Journal of Modern Physics: Conference Series* **19** 417-23 World Scientific Publishing Company
[11] Lenarcic M, Bauer C, Giese M and Jung A 2016 Prediction of S-shaped characteristics in reversible pump-turbines using different numerical approaches *IOP Conference Series: Earth and Environmental Science* **49**(4) 042009. IOP Publishing
[12] Li J, Hu Q, Yu J and Li Q 2013 Study on S-shaped characteristic of Francis reversible unit by on-site test and CFD simulation *Science China Technological Sciences* **56** (9) 2163-9
[13] Yan J P, Seidel U and Koutnik J 2012 Numerical simulation of hydrodynamics in a pump-turbine at off-design operating conditions in turbine mode *IOP conference series: Earth and Environmental Science* **15**(3) 032041. IOP Publishing
[14] Sun H, Xiao R, Wang F, Xiao Y and Liu W 2015 Analysis of the pump-turbine S characteristics using the detached eddy simulation method *Chinese Journal of Mechanical Engineering* **28** (1) 115-22
[15] Xia L, Cheng Y, Yang Z, You J, Yang J and Qian Z 2017 Evolutions of Pressure Fluctuations and Runner Loads During Runaway Processes of a Pump-Turbine *Journal of Fluids Engineering* **139**(9) 091101